Correcting photoacoustic signals for fluence variations using acousto-optic modulation

K. Daoudi, A. Hussain, E. Hondebrink, and W. Steenbergen*

Biomedical Photonic Imaging group, MIRA Institute for Biomedical Technology and Technical Medicine, University of Twente, PO Box 217, 7500 AE Enschede, The Netherlands

**w.steenbergen@utwente.nl*

Abstract: We present a theoretical concept which may lead to quantitative photoacoustic mapping of chromophore concentrations. The approach supposes a technique capable of tagging light in a well-defined tagging volume at a specific location deep in the medium. We derive a formula that expresses the local absorption coefficient inside a medium in terms of noninvasively measured quantities and experimental parameters and we validate the theory using Monte Carlo simulations. Furthermore, we performed an experiment to basically validate the concept as a strategy to correct for fluence variations in photoacoustics. In the experiment we exploit the possibility of acousto-optic modulation, using focused ultrasound, to tag photons. Results show that the variation in photoacoustic signals of absorbing insertions embedded at different depths in a phantom, caused by fluence variations of more than one order of magnitude, can be corrected for to an accuracy of 5%.

OCIS codes: (110.5125) Photoacoustics; (170.6935) Tissue characterization; (170.1065) Acousto-optics.

References and links

1. L. V. Wang, *Photoacoustic Imaging and Spectroscopy* (CRC Press, 2009).
2. J. R. Rajian, P. L. Carson, and X. D. Wang, "Quantitative photoacoustic measurement of tissue optical absorption spectrum aided by an optical contrast agent," Opt. Express **17**(6), 4879–4889 (2009).
3. A. Rosenthal, D. Razansky, and V. Ntziachristos, "Quantitative optoacoustic signal extraction using sparse signal representation," IEEE Trans. Med. Imaging **28**(12), 1997–2006 (2009).
4. R. J. Zemp, "Quantitative photoacoustic tomography with multiple optical sources," Appl. Opt. **49**(18), 3566–3572 (2010).
5. B. T. Cox, S. R. Arridge, and P. C. Beard, "Estimating chromophore distributions from multiwavelength photoacoustic images," J. Opt. Soc. Am. A **26**(2), 443–455 (2009).
6. B. T. Cox, S. R. Arridge, K. P. Köstli, and P. C. Beard, "Two-dimensional quantitative photoacoustic image reconstruction of absorption distributions in scattering media by use of a simple iterative method," Appl. Opt. **45**(8), 1866–1875 (2006).
7. J. Laufer, B. Cox, E. Zhang, and P. Beard, "Quantitative determination of chromophore concentrations from 2D photoacoustic images using a nonlinear model-based inversion scheme," Appl. Opt. **49**(8), 1219–1233 (2010).
8. L. Yao, Y. Sun, and H. B. Jiang, "Transport-based quantitative photoacoustic tomography: simulations and experiments," Phys. Med. Biol. **55**(7), 1917–1934 (2010).
9. L. Yin, Q. Wang, Q. Z. Zhang, and H. B. Jiang, "Tomographic imaging of absolute optical absorption coefficient in turbid media using combined photoacoustic and diffusing light measurements," Opt. Lett. **32**(17), 2556–2558 (2007).
10. Z. Yuan, Q. Wang, and H. B. Jiang, "Reconstruction of optical absorption coefficient maps of heterogeneous media by photoacoustic tomography coupled with diffusion equation based regularized Newton Method," Opt. Express **15**(26), 18076–18081 (2007).
11. A. Q. Bauer, R. E. Nothdurft, T. N. Erpelding, L. V. Wang, and J. P. Culver, "Quantitative photoacoustic imaging: correcting for heterogeneous light fluence distributions using diffuse optical tomography," J. Biomed. Opt. **16**(9), 096016 (2011).
12. X. Q. Li, L. Xi, R. X. Jiang, L. Yao, and H. B. Jiang, "Integrated diffuse optical tomography and photoacoustic tomography: phantom validations," Biomed. Opt. Express **2**(8), 2348–2353 (2011).
13. L. H. Wang, S. L. Jacques, and X. M. Zhao, "Continuous-wave ultrasonic modulation of scattered laser light to image objects in turbid media," Opt. Lett. **20**(6), 629–631 (1995).
14. L. V. Wang, "Mechanisms of ultrasonic modulation of multiply scattered coherent light: an analytic model," Phys. Rev. Lett. **87**(4), 043903 (2001).

#166539 - $15.00 USD Received 12 Apr 2012; revised 1 Jun 2012; accepted 3 Jun 2012; published 11 Jun 2012

15. X. A. Xu, H. L. Liu, and L. V. Wang, "Time-reversed ultrasonically encoded optical focusing into scattering media," Nat. Photonics **5**(3), 154–157 (2011).
16. L. H. Wang, S. L. Jacques, and L. Q. Zheng, "Mcml - monte-carlo modeling of light transport in multilayered tissues," Comput. Meth. Prog. Biol. **47**(2), 131–146 (1995).
17. M. Gross, P. Goy, and M. Al-Koussa, "Shot-noise detection of ultrasound-tagged photons in ultrasound-modulated optical imaging," Opt. Lett. **28**(24), 2482–2484 (2003).
18. A. Bratchenia, R. Molenaar, T. G. van Leeuwen, and R. P. H. Kooyman, "Acousto-optic-assisted diffuse optical tomography," Opt. Lett. **36**(9), 1539–1541 (2011).
19. A. R. Selfridge, "Approximate material properties in isotropic materials," IEEE Trans. Sonics Ultrason. **32**(3), 381–394 (1985).
20. M. Lesaffre, F. Jean, A. Bordes, F. Ramaz, E. Bossy, A. C. Boccara, M. Gross, P. Delaye, and G. Roosen, "Sub-millisecond in situ measurement of the photorefractive response in a self adaptive wavefront holography setup developped for acousto-optic imaging," Proc. SPIE **6086**, 8612 (2006).
21. Y. Z. Li, P. Hemmer, C. H. Kim, H. L. Zhang, and L. V. Wang, "Detection of ultrasound-modulated diffuse photons using spectral-hole burning," Opt. Express **16**(19), 14862–14874 (2008).

1. Introduction

Photoacoustic imaging (PAI) is a biomedical imaging modality of rapidly increasing impact. PAI provides images of turbid media, based on ultrasonic waves created inside the medium by local absorption of short light pulses. The underlying effect is photoelastic energy conversion: local absorption of short light pulses leads to a mechanical stress which relaxes by the emission of ultrasonic waves. From these waves, the initial stress distribution can be reconstructed, which leads to three dimensional imaging of optical absorption. PAI has been elaborated into various implementations, mainly leading to devices for various imaging depths and imaging resolutions [1].

While PAI provides images related to optical absorption it is inherently unable to render quantified images of the absorption coefficient. This is related to the fact, that under the conditions of heat and stress confinement, the initial stress distribution $\sigma(x,y,z)$ depends on the distribution of absorbed energy density E_a as $\sigma = \Gamma E_a = \Gamma \mu_a F = \Gamma F c \varepsilon_a$ with Γ the Grüneisen parameter, μ_a the local absorption coefficient, F the local fluence, c the concentration of the chromophore (a single chromophore is assumed) and ε_a its molar absorption. All above quantities vary with position in the tissue. The quantification problem in photoacoustics is to decompose the reconstructed initial stress distribution $\sigma(x,y,z)$ into fluence F and absorption coefficient μ_a.

Different techniques have been investigated to solve this problem. For example, Rajian et al. [2] proposed a technique based on the injection of an absorbing dye with known concentration, whereas Rosenthal et al. [3] take advantage of the property that often fluence and optical absorption vary at widely different length scales. Using multiple optical sources Zemp [4] demonstrate the possibility of non-iterative reconstruction of quantitative photoacoustic images, however the technique requires *a priori* knowledge of bulk optical properties. The most common approach is a combination of photoacoustics with the application of a model of light transport [5-10] which proves its ability in homogeneous medium. Recently a combination was investigated [11, 12] investigated of photoacoustics with diffuse optical tomography using iterative computational models to achieve quantitative absorption and scattering images.

Here we first theoretically describe a methodology which can allow to determine the local absorption coefficient in photoacoustics. The proposed method is based on the combination of photoacoustics and a technique capable of tagging light in a well-defined tagging volume at a specific location deep in the medium. We validate the theory using Monte Carlo simulations for different situations, and we experimentally show the ability of the technique to correct for fluence variations in photoacoustic signals by using acousto-optics [13] as a way to tag light in a known location within the medium. In acousto-optics the optical phase of diffuse light is modulated by focusing an ultrasound wave through the medium. The effect is caused by the vibration of the light scatterers and modulation of the refractive index in the focal zone [14].

#166539 - $15.00 USD Received 12 Apr 2012; revised 1 Jun 2012; accepted 3 Jun 2012; published 11 Jun 2012

2. Theory

Consider points i and j inside or on the surface of a turbid medium, as depicted in Fig. 1. On injection in point i of light at power P_i, through an aperture placed in point j with area A_j and solid opening angle Ω_j an optical power is detected of

$$P_{ij} = A_j \Omega_j P_i \Pr(i, j) \tag{1}$$

Here $Pr(i,j)$ is the probability per unit aperture area and per unit solid angle that a photon starting in i will cross an aperture at point j, following any possible photon trajectory. The fluence rate Φ_{ij} at point j can be written

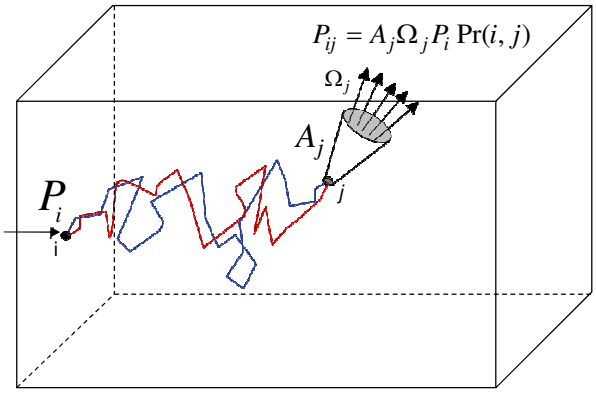

Fig. 1. Schematic of photon trajectories from injection point i to a point j deep in scattering medium. P_i is the injected power and P_{ij} is the power measured at position j through an aperture with area A_j and solid angle Ω_j at point j.

$$\Phi_{ij} = 4\pi P_i \Pr(i, j) \tag{2}$$

the expressions for P_{ij} and Φ_{ij} are in mutual agreement for an assumed isotropic radiance in point j. In an analogous manner, a pulse with pulse energy $E_{p,i}$ applied at surface point i will generate fluence

$$F_{ij} = 4\pi E_{p,i} \Pr(i, j) \tag{3}$$

Probability $Pr(i,j)$ is affected by the unknown optical properties of that part of the medium that is interrogated by the light travelling from i to j. A key aspect of our method is that we exploit the principle that all photon trajectories contributing to $Pr(i,j)$ can be followed in both directions with equal probability, hence $Pr(i,j) = Pr(j,i)$. Photon reversibility has been recently used in an extreme form by Xu et al. [15] for refocusing ultrasound-tagged photons in a scattering medium to the point of tagging, a process which involves both the phase and amplitude of the light. In our use of light reversibility we only use the intensity aspect of light and no phase conjugation is needed.

These principles are now applied to the medium depicted in Fig. 2, with surface points 1 and 3 and a volume around an internal point 2 with absorption coefficient $\mu_{a,2}$. The absorbed energy density at point 2 is

$$E_{a,i2} = F_{i2} \mu_{a,2} = 4\pi E_{p,i} \Pr(i, 2) \mu_{a,2} \tag{4}$$

#166539 - $15.00 USD Received 12 Apr 2012; revised 1 Jun 2012; accepted 3 Jun 2012; published 11 Jun 2012

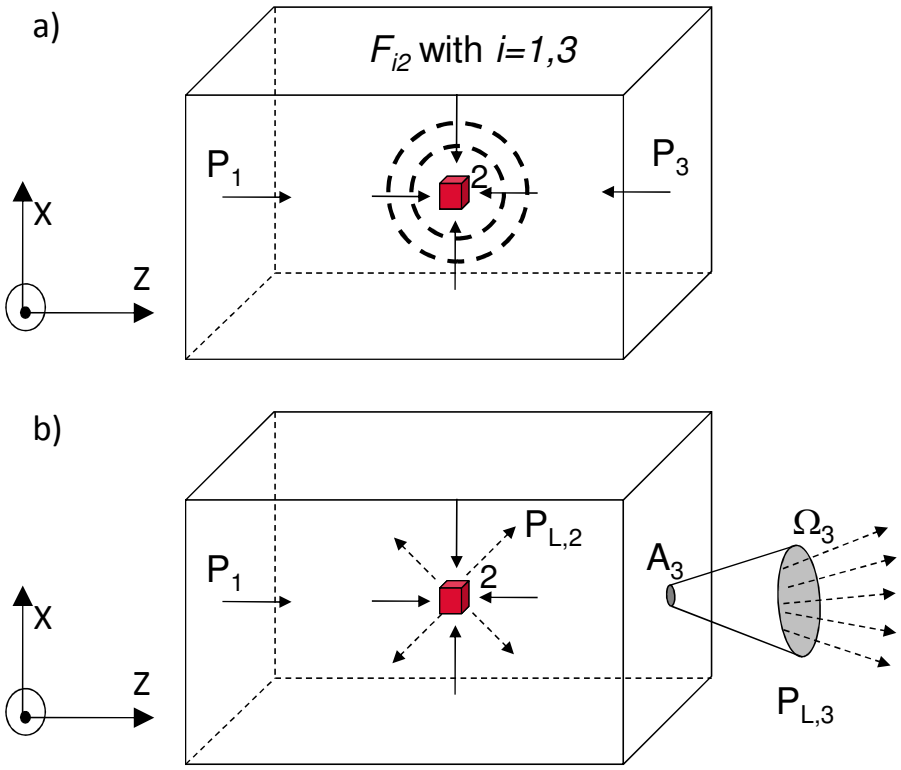

Fig. 2. a) Stress generation in internal point 2 as a consequence of light absorption, with light injection in surface points i = 1 or 3 (solid arrows), leading to F_{i2} fluence in point 2. b) $P_{L,3}$ the detected part of light $P_{L,2}$ labeled at point 2 (dashed arrows) in response to the injected power P_1. Detection is through an aperture A_3 and solid angle Ω_3.

with $i = 1,3$ for injection of light at points 1 and 3, respectively. Here we used Eq. (3) relating the internal fluence to the injected pulse energy. Under the condition of stress confinement, this leads to local stresses

$$\sigma_{2i} = \Gamma F_{i2} \mu_{a,2} = 4\pi\Gamma E_{p,i} \Pr(i,2) \mu_{a,2} \tag{5}$$

for i = 1,3, which are the result of photoacoustic tomography experiments with excitation at points 1 and 3. Around point 2 a volume V_2 is defined in which a known fraction of photons that address this volume are 'tagged'. Here a unit tagging efficiency is assumed. Assuming an incoming fluence rate Φ_{i2} and neglecting absorption, the power of labeled photons re-injected in the medium is then

$$P_{L,i2} = \Phi_{i2} A_2 = 4\pi P_i \Pr(i,2) A_2 \tag{6}$$

with A_2 the average frontal area of volume 2, with averaging over all possible orientations. Here we used Eq. (2) relating the internal fluence rate to the power injected at the medium surface. The internally injected stream of 'tagged' photons at power $P_{L,i2}$ gives rise to detection of 'tagged' photons within an area A_j and solid opening angle Ω_j at point j, at a power that with the use of Eq. (1) can be written

$$P_{L,i2j} = 4\pi P_i \Pr(i,2) \Pr(2,j) A_2 A_j \Omega_j \tag{7}$$

with *(i,j) = (1,3)* or *(i,j) = (3,1).*

#166539 - $15.00 USD Received 12 Apr 2012; revised 1 Jun 2012; accepted 3 Jun 2012; published 11 Jun 2012

Here we assume that tagging of light is restricted to volume 2. Following Eq. (7), the tagging in volume 2 of light injected in point 1, and detected in point 3, leads to

$$P_{L,123} = 4\pi P_1 \Pr(1,2)\Pr(2,3) A_2 A_3 \Omega_3 \tag{8}$$

By applying Pr(2,3) = Pr(3,2), and combining Eq. (5) with $i = 1,3,$ and Eq. (8), we can obtain an expression for the absorption coefficient,

$$\mu_{a,2} = \frac{1}{\Gamma}\sqrt{\frac{A_2 A_3 \Omega_3}{4\pi}}\sqrt{\frac{P_1}{E_{p,1}E_{p,3}}}\sqrt{\frac{\sigma_{21}\sigma_{23}}{P_{L,123}}} \tag{9}$$

This expression for the local absorption coefficient contains only instrumental geometrical parameters (under the first square root), excitation parameters (under the second) and externally measurable quantities (the third square root). The combination of two photoacoustic experiments with injection at two points, and one experiment which allows to tag light at a given location, and with the optodes coinciding with the photoacoustic injection points leads to the elimination of the probabilities *Pr(i,j)* associated with the unknown absorption and scattering properties of the medium. Hence the unknown potentially inhomogeneous optical properties of the tissue, are removed from the problem.

3. Monte Carlo modeling

We give numerical evidence of the potential of our method to measure absorption coefficients without knowledge of the optical properties of the medium. We used a Monte Carlo simulation based on the program by Wang and Jacques [16], with modifications allowing to tag photons addressing a certain volume.

The local thermo-elastic stress was replaced by the number of photons absorbed in a predefined sphere around point 2. In this way, simulation of a full photoacoustic experiment is not required. All photons addressing and escaping this sphere were counted as 'tagged' as assumed in the theory. The sphere is placed in a cubical medium with sides 20mm, having homogenous absorption and scattering properties except for the sphere. The medium is successively illuminated at two surface points for recording the absorbed energy in the sphere, while for tagging only one of these injection points is used, with the other point hosting the light detection window. 10^8 photons were injected through a circular window of 2mm diameter. The 'tagged' photons were detected in a circular window of 2mm diameter and full opening angle of 50 degrees. In the Monte Carlo simulation the estimation of the absorption coefficient of the sphere is performed with an equivalent of Eq. (9) that reads

$$\mu_{a,2} = \sqrt{\frac{A_2 A_3 \Omega_3}{4\pi V_2^2}}\sqrt{\frac{E^*_{a,12}E^*_{a,32}}{P^*_{L,3}}} \tag{10}$$

with V_2 the volume of the absorbing and tagging sphere around point 2, $E_{a,i2}$ is now the number of photons absorbed in the volume, and * denotes normalization with the number of injected photons.

#166539 - $15.00 USD Received 12 Apr 2012; revised 1 Jun 2012; accepted 3 Jun 2012; published 11 Jun 2012

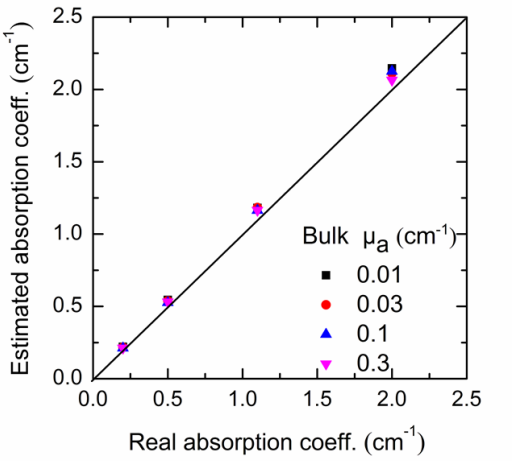

Fig. 3. Estimation of the absorption coefficient in a symmetrically placed absorbing sphere with diameter 2mm, vs. the real absorption coefficient, for a range of bulk absorption levels and a reduced bulk scattering coefficient of 5 cm^{-1}; the medium is a 2*2*2 cm^3 optically homogeneous object. The solid line represents perfect estimation.

Initially the sphere is placed in the center of the medium, and both the absorption coefficient of the sphere and the bulk are varied. Figure 3 shows the estimated vs. the real absorption coefficient, for a range of bulk absorption coefficients within a sphere placed in the center of the medium. The estimation gives an error less than 8%, with always a positive bias. In this simulation, the local fluence due to variations of the bulk properties varied with a factor 2.2

To study the effect of a large variation of fluence levels, both the depth and the lateral position of the sphere was varied, while the optical properties of the bulk and the sphere were kept constant. Figure 4(b) shows the estimated absorption coefficient when the volume is shifted from the illumination point at the surface towards the center (black circles Fig. 4(a)), and from the center towards one of the lateral boundaries (red circles Fig. 4(a)). The absorption is correctly estimated with an error less than 10%, mainly involving an overestimation except when the absorber is close to the illumination point. Figure 4(c) shows the total absorbed energy, equivalent to $\mu_a \Phi V_2$, which varies with a factor of 100. Hence in a photoacoustic experiment with perfect reconstruction of the initial stress, the absorber position variation would lead to fluence variations and therefore image value variations of 2 orders of magnitude. The correction method described by our theory is able to cope with these large fluence variations.

#166539 - $15.00 USD Received 12 Apr 2012; revised 1 Jun 2012; accepted 3 Jun 2012; published 11 Jun 2012

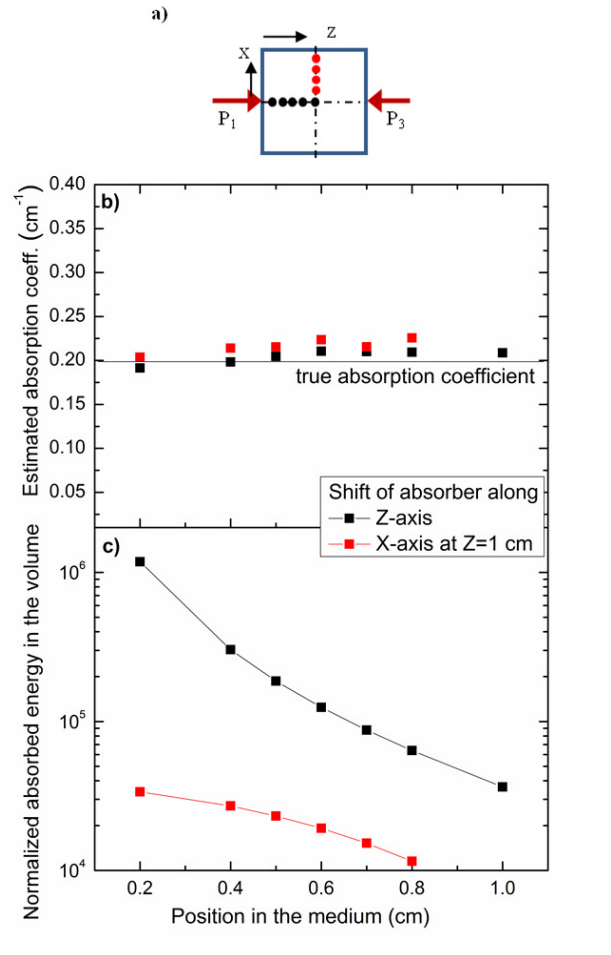

Fig. 4. (a) Schematic of different absorber positions deep in the medium for both directions. (b) Estimated absorption coefficient in a 2mm sphere shifting along the x- and z-axis. (c) The associated absorbed energy for injection in point 1, normalized with the number of injected photons, and equivalent to $\mu_a \Phi V_2$ and representing photoacoustic image levels, varies with 2 orders of magnitude.

4. Experimental validation

To achieve quantification using the presented method, we experimentally need to locally tag photons. Acousto-optic modulation of light [13] is a technique allowing to label light in a specific location. However, unlike the assumptions in our theory, the tagging efficiency is less than one and the tagging volume is a focused ultrasound field of complicated shape.

The objective of the experimental study in this work is to validate the concept of combining photoacoustics and acousto-optics as a strategy to correct for fluence variation in photoacoustic signals. For this purpose, we simplify Eq. (9) to relax a few of its requirements. If the sample is highly scattering with identical absorbing insertions at different depths, we can assume that the Grüneisen parameter and all geometrical parameters, including the active frontal area A_2 of the tagging volume Eq. (9), are constant. The optical excitation of the phantom during the measurements can also be merged into a constant factor and as a result Eq. (9) can be written as,

#166539 - $15.00 USD Received 12 Apr 2012; revised 1 Jun 2012; accepted 3 Jun 2012; published 11 Jun 2012

$$\mu_{a,2} = C\sqrt{\frac{p_{21}p_{23}}{P_{L,13}}} \tag{11}$$

where p_{21} and p_{23} are the measured photoacoustic pressures generated by a local absorber in internal point 2 by illuminating at position 1 and 3 respectively and $P_{L,13}$ is the power of ultrasonically modulated light (being modulated at position 2) detected at position 3 when the medium is illuminated at position 1. Hence we assume that these externally measured pressures are linked in a linear manner to the photoelastic stresses σ_{21} and σ_{23} inside the absorbers, which has to be assured by a correct experimental design. The purpose of this experiment is to demonstrate that for multiple identical insertions, regardless of their depth inside the turbid phantom, it is possible to get the same relative absorption coefficient value from all the insertions, by assuming that C in Eq. (11) has the same value for each insertion (which will be true for identical insertions). The experimentally measured value using Eq. (11) is proportional to the absorption coefficient.

The experiments were performed on a phantom consisting of a scattering cylinder with a diameter of 20 mm made of a 2% agar gel containing a dilution of 4% intralipid (20%IL). The sample contains three identical nylon fishing threads with thickness of 300 μm inserted at 6, 10, and 14 mm under the surface of the cylinder shown in Fig. 5.

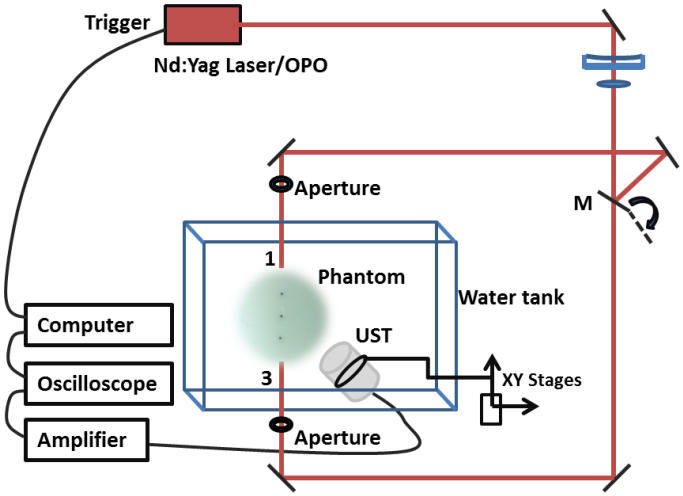

Fig. 5. Schematic of PA Set-up (top view). M: flipping mirror, L: lens and UST: Ultrasound transducer.

The schematic of the PA set-up is shown in Fig. 5. It comprises a frequency doubled Nd:YAG laser (Brilliant B, Quantel Paris) equipped with an OPO system delivering 44 mJ/cm^2 per pulse at 760 nm wavelength, with a duration of 6 ns and a beam diameter of 5 mm. The sample can be illuminated at point 1 by mirror M in the path of the beam and at point 3 by flipping mirror M out of the beam path. PA signals were detected with a single element 5MHz focused ultrasound transducer (Panametrics V309) oriented at 45° to the line along the absorbers, and attached to a linear xy translation stage (MTS50-Z8) which allowed precise scanning of the US focus along a line through the absorbers. The oblique angle was chosen instead of 90° to prevent partly overlap of the signals of the three absorbers. The linear transducer scan parallel to the absorbing objects ensures that the distance from each absorber to the transducer, when in focus, is identical. Hence *1/r* decay and frequency dependent attenuation are constant, and hence we can expect the pressure amplitude p to be proportional to the photoelastic stress σ inside each absorber. Both sample and UST were immersed in water for acoustic coupling, the PA signal from UST was amplified using Panametric

#166539 - $15.00 USD Received 12 Apr 2012; revised 1 Jun 2012; accepted 3 Jun 2012; published 11 Jun 2012

NDT(5077PR) amplifier and sent to an oscilloscope (Textronix TDS 220) which was triggered by the laser and a computer was used to read and store the data from oscilloscope.

For the acousto-optic measurements we used a Ti:sapphire laser (Coherent MBR110) pumped by a solid state laser at 532 nm (Verdi, Coherent). The sample was illuminated by a laser beam (diameter of 5 mm, power of 650 mW) at wavelength of 760 nm. Local light tagging was done with 5MHz focused ultrasound transducer (Panametrics V309, diameter of 12.7mm and focal length of 20.3mm), giving pulses of 1 microsecond duration which lead to a spatial resolution of 0.4 mm in the transversal plan and 1.5 mm in the axial direction. The signal was amplified using (ENI 350L power amplifier) leading to a pressure of 1MPa at the focal zone. Ultrasonically tagged light was detected using the two phase homodyne interferometry principle developed by Gross et al. [17]. The detection window had a size of 5 mm. We used a CCD camera with a 30 Hz frame rate, running at 3.5 ms exposure time to record the digital hologram. The details of this setup can be found elsewhere [18].

Figure 6(a) and 6(b) show peak to peak values of the PA signal for 3 insertions versus their depth inside the phantom, whereas the inset graphs show the PA signal versus its arrival time at the US transducer for insertion 1, 2 and 3 by illuminating the sample at position 1 and 3 respectively. Each PA signal is averaged over 128 light pulses, whereas error bars on peak to peak values are obtained by taking standard deviation of six such independent PA measurements. The local fluence for the identical insertions varies up to a factor 13 as can be seen from the PA signals. The peak-to-peak time from all insertions is identical, which allows neglecting the frequency dependent attenuation. Figure 6(c) shows the AO signal (I_{tagged}) versus the depth of the US focus along the optical axis (where insertions are embedded), for one of the four independent measurements performed on this phantom in transmission mode. During the AO measurement the sample was illuminated at point 1 and the ultrasonically modulated light was detected at point 3, where the light was modulated by scanning the US focus in steps of 0.5 mm along the line through the embedded insertions. This AO signal is averaged over 8 ultrasound pulses, where each pulse consists of 5 ultrasound cycles. The dips in the AO signal curve are due to the presence of insertions which match with expected locations of insertions. Figure 6(d) shows the estimated relative absorption coefficient normalized by the unknown constant (which is the same for all identical absorbers) for different insertions using Eq. (11). To obtain this relative absorption coefficient for all insertions using Eq. (11), we used the peak-to-peak values of PA signals (p_{21} and p_{23}) for each insertion from Fig. 6(a) and Fig. 6(b) and the AO signal ($P_{L,13} \propto I_{tagged}$) coming from the location of corresponding absorbing insertions indicated with arrows in Fig. 6(c). The AO values used in Eq. (11) to calculate the relative absorption coefficient are the lowest values in the dips of AO curve caused by the presence of insertions, and are pointed by arrows in Fig. 6(c). The error bars shown in Fig. 7(d) are based on estimation of error propagation due to noise present in multiple independent AO and PA measurements. The estimation of noise (uncertainty) is done by taking the standard deviation of multiple AO and PA measurements.

As we can see, the estimated values are the same for all insertions regardless of their positions in the phantom. Hence a fluence variation of a factor 13 has been compensated with an accuracy of 5%.

#166539 - $15.00 USD Received 12 Apr 2012; revised 1 Jun 2012; accepted 3 Jun 2012; published 11 Jun 2012

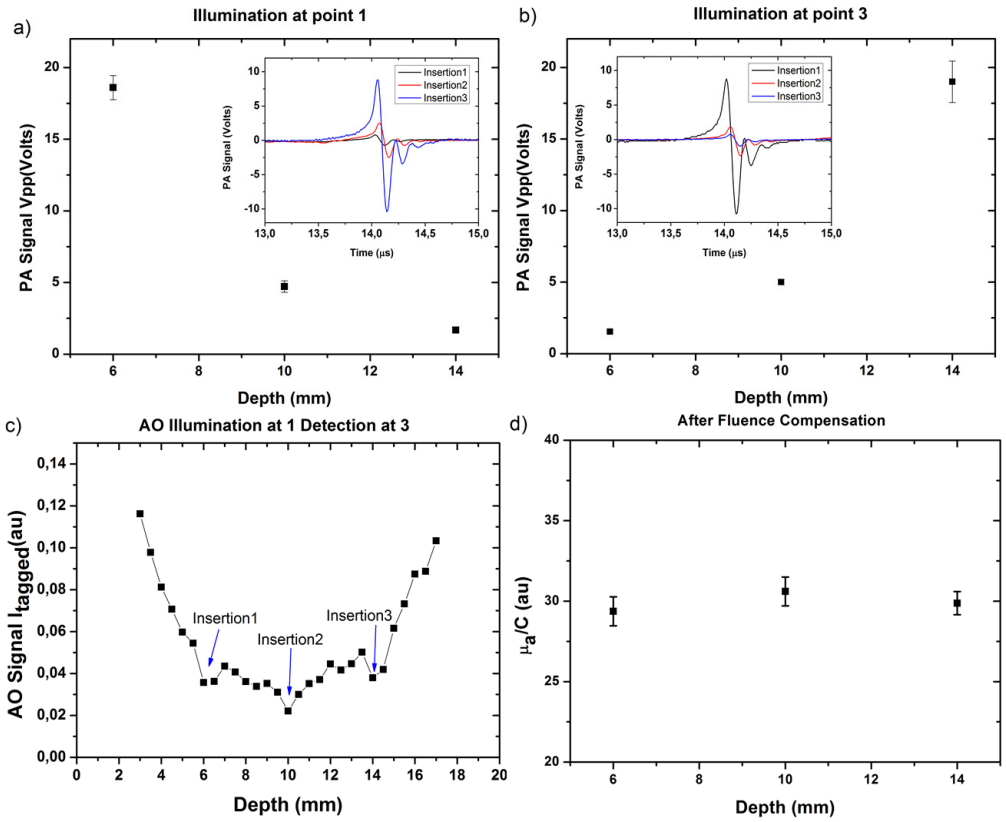

Fig. 6. (a) peak to peak values of PA signal from insertions vs. their depth in phantom for excitation at position 1. (b) peak to peak values of PA signal from insertions vs. their depth in phantom for excitation at position 3. The insets are the detected PA signals for different insertions. (c) AO signal along the line of insertions when light is injected at point 1 and detected at point 3. (d) relative absorption coefficient for all insertions obtained by using Eq. (11).

For further validation of our methodology to compensate for fluence heterogeneities in PA images using AO modulation, we performed another experiment where embedded absorbing inclusions inside the scattering medium had different levels of absorption. This tissue phantom was a scattering cube of 3x3x3 cm^3, made with 2% agar gel containing a dilution of 3% intralipid (20%IL). This sample contains two nylon tubes with 0.94 mm and 0.75 mm outer and inner diameter respectively, inserted at 10 mm and 22 mm depth from the illuminated surface 1. We prepared two absorbing solutions, solution 1 was made with 30 µl India ink dissolved in 10 ml water whereas solution 2 was made with 10 µl India ink dissolved in 10 ml water. Measurements with a spectrophotometer showed that solution 1 and solution 2 have absorption coefficients of 1.5/mm and 0.45/mm respectively at 532 nm wavelength. Tube 1 positioned at depth of 10 mm inside phantom was filled with absorbing solution 1, whereas tube 2 positioned at depth of 22 mm inside the phantom was filled with absorbing solution 2.

We performed two photoacoustic measurements and an acousto-optic measurement using experimental parameters and procedures as in the previous set of experiments, except that both the pulsed (for PA) and continuous wave (for AO) lasers were operating at 532 nm wavelength delivering 9 mJ/pulse and 700 mW respectively through an aperture of 5 mm diameter in both cases. The results of these experiments are shown in Fig. 7. Figures 7(a) and 7(b) show peak-to-peak values of PA signal coming from tube 1 and tube 2 when the sample is illuminated at 1 and 3 respectively, whereas Fig. 7(c) shows the AO signal ($P_{L,13}$ α I_{tagged})

#166539 - $15.00 USD Received 12 Apr 2012; revised 1 Jun 2012; accepted 3 Jun 2012; published 11 Jun 2012

when the sample is illuminated at 1 and ultrasonically modulated light is detected at 3. Figure 7(d) shows the estimated relative absorption coefficient normalized by unknown constant C (μ_a/C) of solutions contained in both nylon tubes. The values of the relative absorption coefficient are obtained using Eq. (11) in the same way as before. The error bars shown in Fig. 7(d) are based on estimation of error propagation due to noise present in multiple independent AO and PA measurements.

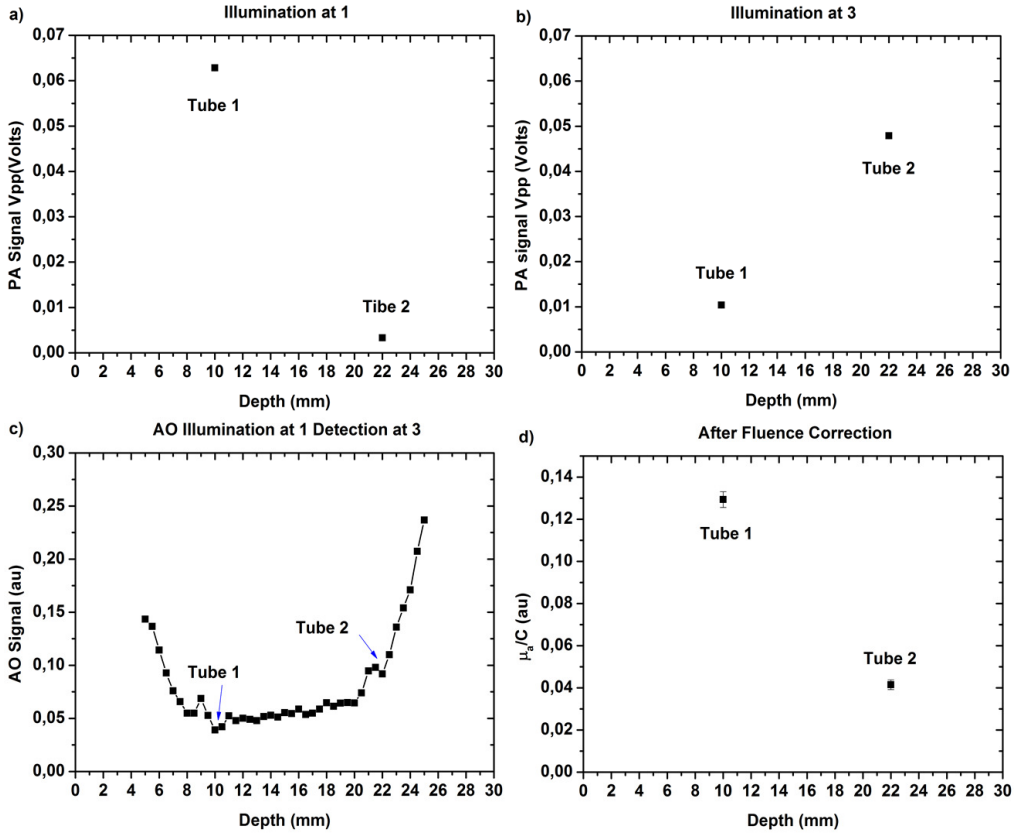

Fig. 7. (a-b) peak to peak values of PA signal from tubes vs. their depth in phantom for excitation at position 1 and 3, respectively. (c) AO signal along the straight line between injected point at 1 and detection point at 3. (d) relative absorption coefficient for solutions contained in tube 1 and 2 obtained by using Eq. (11).

The results in Fig. 7(d) show that the ratio between the relative absorption coefficient of solution 1 in tube 1 to solution 2 in tube 2 is 3.118 ± 0.194. This ratio of estimated relative absorption coefficients of these solutions matches with the photo-spectroscopic measured ratio of absorption coefficients for these solutions, which is 3.3 with an inaccuracy of 5.7%. Hence our experimental results show that at least for the range of absorption coefficients considered here we can correct photoacoustic signals due to fluence variations with the help of local AO modulation of light.

5. Discussion and conclusion

We presented a theory which suggests a method for quantifying the absorption coefficient in highly scattering media by photoacoustics. The approach assumes idealized tagging of light addressing a well-defined volume at a specific location in the medium with unit efficiency. A relationship Eq. (9) is derived that expresses the local absorption coefficient in terms of two reconstructed PA image values obtained with two different light injection points, the detected power of light tagged in the internal point of interest, and system parameters. The illumination

#166539 - $15.00 USD Received 12 Apr 2012; revised 1 Jun 2012; accepted 3 Jun 2012; published 11 Jun 2012

and detection points for the tagging experiment should coincide with the two injection points of the PA experiment. Prior knowledge regarding the optical properties of the medium is not required. The main assumption underlying our theory is that photons injected at 1 and reaching an internal tissue location in a certain direction are proportionally represented by photons injected at 3 and reaching the same location in the opposite direction. This is realized if the irradiances $\boldsymbol{I}_{12}(\boldsymbol{s})$ and $\boldsymbol{I}_{32}(\boldsymbol{s})$ in point 2 are each other's point mirrored version, which will generally be the case for multiply scattered light which creates almost isotropic radiances. Close to light sources, tissue boundaries or strong inhomogeneities and by shadowing of a neighboring absorbing volume, this condition might break down.

Simulations give absorption estimations which are correct within a maximum overestimation of 10%, for fluence variations of two orders of magnitude. The dominantly positive bias has various causes which are related to the size of the labeling volume. Our assumption of an absorbed energy in probing volume V_2 equal to $\mu_a \Phi V_2$ only holds if the linear dimensions of the volume are smaller than $1/\mu_a$ and a length scale between $1/\mu_s$ and $1/\mu_s'$. The overestimation is also caused by the absorption of tagged photons in the labeling volume. In fact, the fluence of tagged photons escaping from the volume at point 2, described by Eq. (6), is lower than the amount of light entering the volume because of the absorption. This missing amount of light is even more pronounced when the labeling volume is bigger and absorption coefficient is higher. For more accuracy this effect should be taken into account in Eq. (6) by subtracting the absorbed amount of energy. However, for a small labeling volume the effect is negligible.

We performed two experiments to basically validate the concept as a strategy for correcting photoacoustic signals for fluence variations throughout the medium. In these experiments we used the acousto-optic technique as a way to tag photons in a specific location. Results show that the variation in photoacoustic signals as caused by fluence variations has been corrected at an accuracy of 5%. The peak-to-peak times of the bipolar signals of the three absorbing objects (Fig. 6(a) and 6(b)) in the first experiment are identical, indicating that frequency dependent attenuation, if any, has affected the signals to an equal amount. Hence it is safe to assume that the bipolar signal amplitudes are proportional to the original photoelastic stresses inside the absorbers. The possible contributing factors to the local minima in AO signal at insertion locations (Fig. 6(c), Fig. 7(c)) can be optical absorption in the insertion and their acoustic impedance mismatch between nylon (3.14MPa.s/m [19]) and water, 1.48 MPa.s/m). This impedance mismatch can affect the estimation of tagged signal, by affecting the tagging efficiency. However, this wouldn't affect our results as far as we are using the same type of insertions, which allows us to merge the tagging efficiency into the constant C in Eq. (11). In the second experiment we used nylon tubes filled with two different ink solutions with a ratio of absorption coefficients of 3.3. Results showed further evidence of the potential of our technique to achieve fluence-corrected photoacoustic measurements by estimating relative absorption coefficients with a ratio of 3.1 between the absorbers using Eq. (11). The technique in its current stage can be used for example to correct the effect of wavelength-dependence of the photoacoustic signal in spectroscopy without use of any computational model.

Combining photoacoustics and acousto-optics may bring experimental absolute optical absorption imaging closer. However, the presented theory needs to be elaborated. Further work will focus on bridging the gap between the simple discrete labeling volume with unit tagging efficiency presented in the theory and the simulations, and the physically real ultrasound focus which is soft, of complicated shape and with a small tagging efficiency. In fact, both volume and efficiency can be affected by many parameters as acoustic attenuation, tissue type at the focal region, and coupling of US and tissue. Also, acousto-optic signals generally suffer from high noise levels. This is especially true in vivo where tissue motion can cause optical speckle decorrelation. Many detection techniques are investigated by other research groups to overcome these problems. Gross et al. [17] has proposed a method to detect tagged photons based on heterodyne parallel speckle detection which allows highly

#166539 - $15.00 USD Received 12 Apr 2012; revised 1 Jun 2012; accepted 3 Jun 2012; published 11 Jun 2012

sensitive detection. Other research groups proposed a detection technique based on a photorefractive crystal with fast response time [20], or by applying a quantum spectral filter based on spectral hole burning [21] which allows to overcome speckle decorrelation. These promising techniques have to prove their ability in vivo. The presented model assumed perfect reconstruction of the initial stresses generated in the medium, which in general will not be an easy task in an experiment. In fact, it depends on many parameters such as acoustic coupling, transducer efficiency, mechanical response, transducer characteristics, and on the availability of sufficient ultrasound data. Therefore, some calibration will be needed to accomplish the absolute quantification.

The eventual goal of the presented approach is quantitative absorption mapping which will allow for quantitative chromophore mapping. This will enable local quantification of natural chromophores such as hemoglobin, e.g. as a result of angiogenic processes or angiogenesis inhibition. Another application is the quantification of targeted contrast agents and the concentration of locally delivered drugs. These applications will be useful in fundamental research, drug development and clinical treatment monitoring. Absolute absorption imaging being our ultimate goal, the intermediate goal of fluence variation compensation, purely based on experiments, is more within reach and very useful in itself.

Acknowledgments

This research was supported by the Technology Foundation in the Netherlands (STW) under vici-grant 10831, by Agentschap NL under Eureka grant E!4993, and by the MIRA Institute of the University of Twente. Robert Molenaar and Jithin Jose are acknowledged for experimental support.

#166539 - $15.00 USD Received 12 Apr 2012; revised 1 Jun 2012; accepted 3 Jun 2012; published 11 Jun 2012